Expanded phase stability of Gd-based garnet transparent ceramic scintillators

Zachary M. Seeley,[a] Nerine J. Cherepy, and Stephen A. Payne
Lawrence Livermore National Laboratory, Livermore California 94550, USA

(Received 15 April 2014; accepted 15 July 2014)

Gadolinium-based transparent polycrystalline ceramic garnet scintillators are being developed for gamma spectroscopy detectors. The scintillator light yield and energy resolution depend on many of the ceramic characteristics, including composition, homogeneity, and presence of secondary phases. To investigate phase stability dependence on composition, three base compositions – $Gd_3Ga_{2.2}Al_{2.8}O_{12}$, $Gd_{1.5}Y_{1.5}Ga_{2.2}Al_{2.8}O_{12}$, and $Gd_{1.5}Y_{1.5}Ga_{2.5}Al_{2.5}O_{12}$ were studied, and for each composition the rare earth content was varied according to the formula $(Gd,Y,Ce)_3(Y_XGa_{1-X})_2(Ga,Al)_3O_{12}$; where $-0.01 < X < 0.05$. We have found that yttrium and gallium help to stabilize the garnet crystal structure in the ceramics by allowing interionic substitution among the cationic garnet sites. Specifically, a composition of $Gd_{1.49}Y_{1.49}Ce_{0.02}Ga_{2.5}Al_{2.5}O_{12}$ can accommodate approximately 2 at.% excess rare earth ions from the perfect garnet stoichiometry and remain a phase pure transparent ceramic with optimal performance as a radiation detector. This expanded phase stability region helps to enable the fabrication of large transparent ceramics from powder with tolerance for flexibility in chemical stoichiometric precision.

I. INTRODUCTION

The development of scintillators for gamma ray spectroscopy requires simultaneous optimization of a variety of properties. Their effective atomic number should be maximized (to effectively interact with ionizing radiation via the photoelectric effect), their light yield under excitation by ionizing radiation (photons/MeV) should be as high as possible (to minimize the effect of photon statistics), their optical clarity should be excellent (for effective and homogeneous light collection), and their emission spectra should be in the blue–green range (for high-efficiency photodetection by standard bialkali photomultiplier tubes). Gd-based garnets offer a unique class of materials capable of high performance in this application.

Transparent ceramics offer advantages in low-cost production and large-size uniformity, compared to single crystals. The great success of YAG (yttrium aluminum garnet) transparent ceramics achieving broad commercial implementation inspired our search for a garnet transparent ceramic scintillator that could supplant single crystal dominance in this field. The simple high-*Z* analog of YAG, GAG (gadolinium aluminum garnet) is well known to be difficult to grow due to the limited range of its phase stability; for example, one report of growth of GAG from flux required 25 wt% flux and the small crystals that could be obtained were highly flawed.[1] Generally speaking, single crystals can typically be grown with feedstock that is somewhat off-stoichiometry, since during solidification, the excess can be rejected from the as-formed crystals to the top of the boule, for certain melt-growth methods (such as Bridgman), or left behind in the crucible for others (such as Czochralski). In contrast, transparent ceramics require strict adherence to a stoichiometry that can provide the correct crystal phase for the entire volume. Any off-stoichiometric excess will lead to secondary phases and give rise to optically scattering secondary phase inclusions at grain boundaries. For example, the stoichiometry tolerances for YAG powders used in transparent ceramics fabrication are tight, as it is a line compound. Nonstoichiometric GGAG(Ce) phosphors described in Ref. 2 provided insight into the potential flexibility and relationship between the phase stability of Gd garnets and cationic substitution populations. In this paper, we describe our ongoing efforts to engineer a Gd-based garnet, amenable to transparent ceramics processing, by using the principle of intersubstitutional ions to enhance a broad stoichiometric range over which the garnet phase is stable.

After our results published in 2010, demonstrating the energy resolution for GYGAG(Ce) of R (662 keV) <5%,[3] a breakthrough performance for oxide scintillators, many efforts have been made to explore compositions of Gd-based garnets containing intersubstitutional ions.[4–6] Most reports involve single crystal growth, powder synthesis, and/or computational techniques, and are aimed at identifying high light yield compositions.

[a]Address all correspondence to this author.
e-mail: seeley7@llnl.gov
This paper has been selected as an Invited Feature Paper.
DOI: 10.1557/jmr.2014.235

 © Materials Research Society 2014

https://doi.org/10.1557/jmr.2014.235 Published online by Cambridge University Press

One important optimization involves the Ga content: a higher Ga provides the desirable shorter wavelength emission, but when Ga concentration is too high, the conduction band level is reduced too much, leading to quenching of the Ce^{3+} luminescence.[6]

For a transparent ceramic garnet scintillator for gamma spectroscopy to be commercialized, process conditions must be developed to produce large, homogeneous ceramics, as described in our previous work,[7] and a robust composition that is insensitive to minor process modifications is needed, as addressed in this paper. Here we report on Gd-garnet compositions that are both high light yield, providing excellent gamma ray spectroscopy, and highly phase stable over a broad stoichiometric range, for economical ceramics fabrication. With such compositions, we obtain scintillation providing energy resolution of as good as 4.3% at 662 keV, with photomultiplier tube (PMT) readout, and large-size ceramics (>2 in^3) with high optical transparency.[8] These scintillators may be integrated into gamma spectrometers using PMT or silicon photodiode readout to provide spectroscopy that is superior to that of the standard scintillators, thallium-doped sodium and cesium iodide.[9,10]

II. METHODS

A. Transparent ceramics fabrication

To study the effect of chemical composition on the phase purity of Gd-based garnet ceramics, nanoparticles of the general formula $(Gd,Y,Ce)_3(Ga,Al)_5O_{12}$ were synthesized via the flame spray pyrolysis (FSP) method by Nanocerox Inc. (Ann Arbor, MI). Three distinct garnet compositions were studied: GGAG(Ce) ($Gd_{2.98}Ce_{0.02}Ga_{2.2}Al_{2.8}O_{12}$), GYGAG(Ce) ($Gd_{1.49}Y_{1.49}Ce_{0.02}Ga_{2.2}Al_{2.8}O_{12}$), and $GYG_{2.5}AG(Ce)$ with a higher gallium content ($Gd_{1.5}Y_{1.5}Ga_{2.5}Al_{2.5}O_{12}$). In addition, to study the allowable concentration of intersubstitutional ions, within each of these three garnets the composition of excess rare earth was varied according to the formula $(Gd,Y,Ce)_3(Y_XGa_{1-X})_2(Ga,Al)_3O_{12}$; where $-0.01 < X < 0.05$.

Nanoparticles were suspended in an aqueous solution containing polyethylene glycol (PEG) and ammonium polymethacrylate (Darvan C-N) using an ultrasonic probe and a high shear Thinky mixer. This suspension was spray dried in a Buchi glass chamber, and the resulting powder was uniaxially pressed at 5 ksi followed by a cold isoatatic press (CIP) at 30 ksi to form the ~50% dense green body. Organics were removed by a heat treatment at 900 °C in air. The calcined compacts were then loaded into a Thermal Technology's tungsten element vacuum furnace and sintered under a vacuum of $<2 \times 10^{-6}$ Torr at 1600 °C for 2 h to reach closed porosity and densities of approximately 97%. The sintered samples were then hot isostatically pressed (HIP'ed) under 200 MPa of inert argon gas pressure at 1650 °C for 4 h in an American Isostatic Presses' tungsten element HIP. Since the samples were closed porosity after vacuum sintering, no canning was necessary during the HIP step. Ceramic surfaces were ground, given an inspection polish, and wipe-cleaned with acetone and methanol.

B. X-ray diffraction (XRD)

A Bruker D8 Advance x-ray diffractometer (XRD; Bruker, Madison, WI) equipped with a Cu anode tube operated at 40 kV and 40 mA was used to characterize the polished surfaces of the ceramics. The peak angle for the two most intense peaks was calculated from the center of the full width at half max (FWHM) and used to calculate the lattice parameter.

C. Beta-excited radioluminescence

Radioluminescence spectra were acquired using a $^{90}Sr/^{90}Y$ source (~1 MeV average beta energy). The spectra were collected with a Princeton Instruments's Acton Spec 10 spectrograph coupled to a thermoelectrically cooled silicon charge-coupled device (CCD) camera.

D. Scintillation characterization with PMT readout

The pulse height spectra were measured with a ^{137}Cs source. The samples were optically coupled to a Hamamatsu R6231-100 PMT, which was connected to an Ortec 113 preamplifier, and the signals were shaped with a Tennelec TC 244 spectroscopy amplifier (shaping time of 4 μs; Tennelec, Oak Ridge, TN) and then recorded with an Amptek MCA8000A multichannel analyzer (MCA; Amptek, Bedford, MA). The spectra were analyzed off-line by nonlinear least squares fitting to a Gaussian to estimate the energy resolution. The light yields were measured by comparing the spectra with a standard YAG(Ce) ceramic from Baikowski.

III. RESULTS AND DISCUSSION

A photograph to display the transparency of the polished ceramics fabricated from various powder compositions is shown in Fig. 1. The three different garnet compositions, GGAG(Ce) ($Gd_{2.98}Ce_{0.02}Ga_{2.2}Al_{2.8}O_{12}$), GYGAG(Ce) ($Gd_{1.49}Y_{1.49}Ce_{0.02}Ga_{2.2}Al_{2.8}O_{12}$), and $GYG_{2.5}AG(Ce)$ ($Gd_{1.5}Y_{1.5}Ga_{2.5}Al_{2.5}O_{12}$) are separated by rows, and along each row, the rare earth content is varied according to the formula $(Gd,Y,Ce)_3(Y_XGa_{1-X})_2(Ga,Al)_3O_{12}$, where $-0.01 < X < 0.05$. The samples are lettered for specific reference below. Within each row, the left-most samples (A, G, and N) have the smallest composition of rare earths and are actually made from powder that is off of the perfect garnet stoichiometry. All these samples display some amount of degraded transparency, which is likely due to the deficiency in rare earth ions causing precipitation of a gallium- or an aluminum-rich secondary phase.

https://doi.org/10.1557/jmr.2014.235 Published online by Cambridge University Press

The transparency of the samples improves as the rare earth content is increased (moving to the right along each row), but eventually degrades again at the far right of each row (samples E, L, and V), this time due to a rare earth–rich secondary phase precipitating at the grain. Gallium-containing garnets are well known to have a range of compositional phase stabilities due to the ability of Ga and rare earth ions to substitute each other on different sites, i.e., they are not line compounds in the phase diagram.[11,12] However, the most notable result in this work is that the width of this phase stability region is significantly dependent on the composition of the garnet. In the GGAG(Ce) (top row), this region is limited to only three samples (B,C, and D) which span a stability region of $X = 0$ to $X = 0.01$. When we add yttrium to the garnet to make GYGAG(Ce) (middle row), the stability region widens to four samples. And finally, when we increase the gallium content from $Ga_{2.2}$ to $Ga_{2.5}$ to make $GYG_{2.5}AG(Ce)$ (bottom row), this stability region grows to seven samples (samples O through U) corresponding to the accommodation of 2% excess rare earth ions.

We attribute the varying ranges of phase stability in these materials to the effect of intersubstitutional ions, i.e., the ability for multiple ions to occupy the same lattice sites. The general formula of the garnet's structure has three distinct cationic sites: A, B, and C in the formula $A_3B_2C_3O_{12}$, where A is the 8-fold coordinated dodecahedral site, B is the 6-fold coordinated octahedral site, and C is the 4-fold coordinated tetrahedral site. Due to the different sizes of these sites, there are some size limitations about which metal ions can effectively occupy which sites and form a stable compound. In these compositions, we assume that the large dodecahedral site can only be occupied by the large gadolinium, cerium, or yttrium ions. The octahedral site can most efficiently be occupied by the intermediate-sized yttrium or gallium ions, and the small tetrahedral site can be occupied by the small gallium or aluminum ions. Table I lists the ionic radii of the different cations in the garnet structure substitutional sites.

Following this assumption can explain why we see a difference in the size of the phase stability regions in the different garnets in Fig. 1. In the GGAG(Ce) top row, we do not have yttrium in the garnet and this forces the dodecahedral site to be occupied solely by gadolinium, which, due to its size, is unlikely to occupy any octahedral sites. It is only the gallium and aluminum ions which can participate in the interionic substitution between the octahedral and tetrahedral sites. Limiting the interionic substitution allows the secondary phases to precipitate easily on either end of the compositional spectrum. By adding the yttrium to the garnet in GYGAG(Ce), we have included the possibility for interionic substitution now on all three of the garnet cationic sites. This ionic intersubstitution can allow for a larger deviation from the perfect garnet stoichiometry before secondary phases start to precipitate, thus increasing the phase stability range. The somewhat unanticipated result from Fig. 1 is that with a minimal increase in the gallium content to $GYG_{2.5}AG(Ce)$ (bottom row), the phase stability region grows significantly. This composition should still allow intersubstitutional ions on all the three cationic sites, but it appears that this phase stabilization effect is much more efficient at this gallium content.

To investigate the possible reason for this expanded phase stability region, XRD was performed on a set of the transparent ceramics. Three transparent samples within each of the three garnet compositions were analyzed by XRD: the lowest rare earth content to form transparent samples (samples B, H, and O), moderate rare earth content (samples C, J, and R), and the highest rare earth content to form transparent samples (samples D, K, and U). All peaks for all samples analyzed matched the Gd-based garnet crystal structure and no secondary phases were visible by XRD, consistent with the samples being transparent. However, a close look at the two most intense peaks for each pattern (shown in Fig. 2) reveals some composition-dependent peak shifts. In Fig. 2, the three garnet compositions have been grouped together for

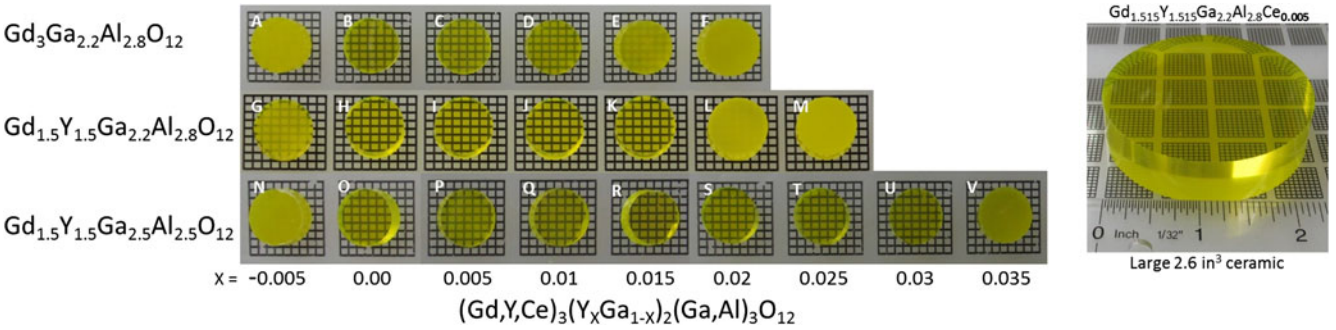


FIG. 1. Photographs of Gd-garnet ceramic samples (3 mm thick) made from powder containing different concentrations of excess rare earths and relative amounts of Ga and Al. Individual samples have been labeled with letters for identification throughout the paper. Right photo is of a 2.6 in^3 transparent ceramic GYGAG(Ce).

https://doi.org/10.1557/jmr.2014.235 Published online by Cambridge University Press

easier interpretation. In the GGAG(Ce) garnet (bottom of Fig. 2), only a slight peak shift to lower angles occurs as the rare earth content increases. This result is consistent with our explanation above considering the limited interionic substitution, leading to a small phase stability region. The dodecahedral and octahedral sites are of fixed sizes with gadolinium and gallium ions respectively, and only the intersubstitution of gallium for aluminum on the tetrahedral site can cause a lattice expansion and a corresponding peak shift.

When yttrium is added to the GYGAG(Ce) (middle patterns of Fig. 2), all the peaks shift to higher angles consistent with a smaller lattice parameter compared with GGAG(Ce), due to the smaller size of the yttrium ion replacing the larger gadolinium ion. In addition, within this group of GYGAG(Ce) ceramics, we notice a significant peak shift to lower angles as the rare earth content increases, indicating a stretching of the lattice parameter. This can only occur due to larger ions being forced onto sites that were previously occupied by smaller ions. As the rare earth content increases, some of the yttrium ions spill over onto octahedral sites, replacing the smaller gallium ions. As this happens, more of the gallium ions have to spill over into the tetrahedral sites and replace the smaller aluminum ions, leading to an overall larger lattice parameter.

When the gallium content is higher, as in $GYG_{2.5}AG$ (Ce) (top patterns of Fig. 2), the peak shift with increased rare earth content is even more pronounced, as is consistent with the broader phase stability region of this material. However, another result from these patterns is that with only a modest (6%) increase in the gallium content relative to the GYGAG(Ce) garnet material, we measure a significant peak shift to lower angles, indicating that we have stretched the lattice parameter. Therefore the increase in the phase stability region for this composition is attributed to the larger lattice parameter allowing for more efficient interionic substitution of larger ions onto smaller sites in which they would

TABLE I. Ionic radii of the cations comprising the gadolinium garnets studied in this work.[13]

Cation	8-fold ionic radius (pm)	6-fold ionic radius (pm)	4-fold ionic radius (pm)
Gd	105	...	...
Ce	114	...	...
Y	102	90	...
Ga	...	62	47
Al	...	53	39

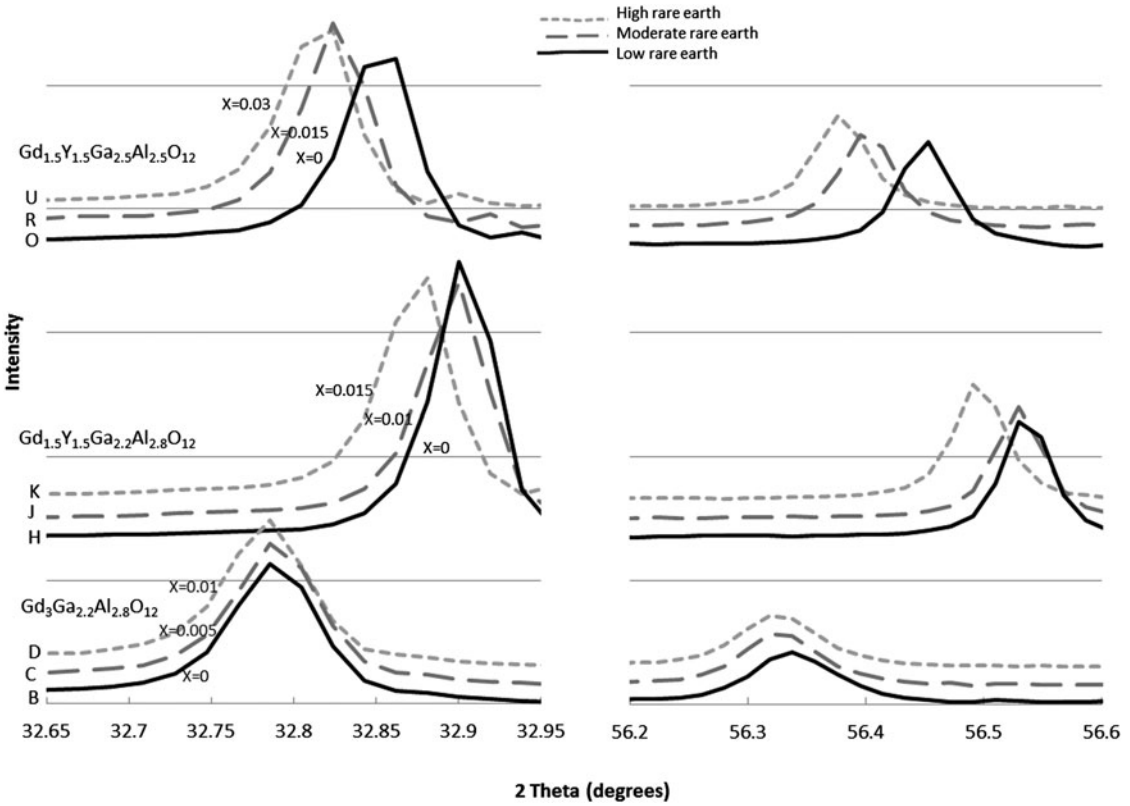


FIG. 2. XRD patterns for the two most intense peaks in the garnet structure. Patterns are grouped together for the three different garnet compositions ($Gd_3Ga_{2.2}Al_{2.8}O_{12}$, $Gd_{1.5}Y_{1.5}Ga_{2.2}Al_{2.8}O_{12}$, and $Gd_{1.5}Y_{1.5}Ga_{2.5}Al_{2.5}O_{12}$), and the line type represents the rare earth content (low, moderate, or high). The patterns have also been labeled using the letters according to the sample identities shown in Fig. 1.

https://doi.org/10.1557/jmr.2014.235 Published online by Cambridge University Press

normally not fit, i.e., more yttrium can spill into the octahedral site and more gallium can spill into the tetrahedral site. For comparison, the lattice parameter of GAG is 12.106 Å.[1]

The XRD peak angles and corresponding lattice parameters are summarized in Table II. To put a quantitative description on the concentration of the interionic substitution that we achieve, X in the formula $(Gd,Y,Ce)_3(Y_XGa_{1-X})_2(Ga,Al)_3O_{12}$ can be calculated from the lattice parameter expansion according to the equation of Brandle and Barns:[12]

$$X = \frac{2\Delta a_0}{1.615(r_{RE} - r_m)} \quad , \qquad (1)$$

where Δa_0 is the stretch in the lattice parameter and r_{RE} and r_m are the weighted average for the ionic radii of the rare earth and the light metal cations (Ga and Al), respectively. The lattice expansion, with increasing rare earth concentration, is calculated from the peak shift for each of the three garnet materials summarized in Table I, and a corresponding X is then calculated from Eq. (1). The concentration of the allowable excess rare earth ions calculated from the XRD data using Eq. (1) is in close agreement with the corresponding sample phase stability regions shown in Fig. 1. Therefore, we can conclude that the compositions described in Fig. 1 are accurate and that the excess rare earth ions can be stabilized in the garnet structure. Because the lattice parameter changes and the material stays in the garnet structure, the compositional phase stability is expanded. For the $GYG_{2.5}AG(Ce)$ composition, this corresponds to allowing an excess of 2% rare earth ions into the garnet structure without secondary-phase precipitation.

In addition to the study of the lattice parameter, radioluminescence spectra provide information on the Ce^{3+} electronic states in the garnet host. The electronic band structure of these related garnets as a function of the composition has been well characterized both theoretically and experimentally.[2,5,14,15] It has been shown that within the garnet structure, increasing the ionic size (i.e., replacing Y with Gd or Al with Ga) tends to both raise the Ce^{3+} excited state as well as reduce the band gap. Our results are consistent with these findings in that increasing the garnet lattice parameter corresponds to blue-shifted Ce^{3+} emission due to the higher excited state. Figure 3 shows that the beta-excited radioluminescence for the Ga = 2.5 composition of $GYG_{2.5}AG(Ce)$ offers the bluest emission of the three compositions described in this paper. The bluer the emission, the better the performance that can be obtained with the standard PMTs used for scintillation counting. However, increasing the lattice parameter too far (i.e., Ce:GGG) will result in nonluminescent recombination and reduced light yield from the scintillator.

For the samples described in Figs. 1 and 3, the scintillation performance, including light yield and energy resolution under gamma ray excitation, was obtained and is shown in Table III. We have previously shown that the uniform Ce-doping levels across the optic due to the solid-state sintering method result in high-performance gamma spectroscopy scintillators.[7] We are developing prototype detectors incorporating GYGAG scintillators, based on both PMT and silicon photodiode readout, since an even better energy resolution of R(662 keV) < 3.5% can be obtained with silicon photodetectors.[8] The initial results obtained with the $Gd_{1.48}Ce_{0.02}Y_{1.5}Ga_{2.5}Al_{2.5}O_{12}$ may be improved upon once we optimize the fabrication for this composition.

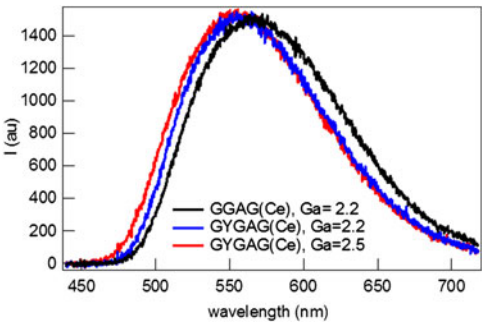


FIG. 3. Radioluminescence spectra of GYGAG(Ce) garnets as a function of the Ga/Al ratio indicate that the emission is blue shifted with additional Ga. In addition, GGAG(Ce), without Y exhibits a red-shifted emission, compared to the GYGAG(Ce) analog.

TABLE II. XRD peak positions and calculated lattice parameters from Fig. 2.

Garnet Composition	Rare earth content (X in Fig. 1)	Peak 1 angle	Peak 2 angle	Average lattice parameter (Å)	Lattice stretch (Δa_0) Eq. 1	X from (Eq. 1)
	0	32.787	56.338	12.2085		
$Gd_3Ga_{2.2}Al_{2.8}O_{12}$	0.005	32.787	56.327	12.2095	0.0015	0.0037
	0.01	32.783	56.326	12.21		
	0	32.9	56.436	12.1685		
$Gd_{1.5}Y_{1.5}Ga_{2.2}Al_{2.8}O_{12}$	0.01	32.896	56.530	12.17	0.009	0.0269
	0.015	32.872	56.496	12.1775		
	0	32.849	56.450	12.186		
$Gd_{1.5}Y_{1.5}Ga_{2.5}Al_{2.5}O_{12}$	0.015	32.823	56.400	12.1955	0.014	0.0361
	0.03	32.812	56.377	12.2		

https://doi.org/10.1557/jmr.2014.235 Published online by Cambridge University Press

TABLE III. Scintillation performance of Gd-garnet transparent ceramics described in this paper.

Composition	Emission peak (nm)	Gamma light yield w/PMT (relative)	Energy resolution w/PMT at 662 keV
$Gd_{2.98}Ce_{0.02}Ga_{2.2}Al_{2.8}O_{12}$	570	1.7	5.0%
$Gd_{1.49}Ce_{0.02}Y_{1.49}Ga_{2.2}Al_{2.8}O_{12}$	560	1.8	4.3% (1 cm^3 size) 4.6% (2 in^3 ceramic)
$Gd_{1.49}Ce_{0.02}Y_{1.49}Ga_{2.5}Al_{2.5}O_{12}$	550	2.0	4.6% (initial 1 cm^3 ceramics)
YAG(Ce) from Baikowski	550	1.0	6.7%

IV. CONCLUSION

Cerium doped gadolinium-based garnet transparent ceramics covering a wide compositional range have been fabricated and characterized for their phase stable region. Three base compositions: $Gd_3Ga_{2.2}Al_{2.8}O_{12}$, $Gd_{1.5}Y_{1.5}Ga_{2.2}Al_{2.8}O_{12}$, and $Gd_{1.5}Y_{1.5}Ga_{2.5}Al_{2.5}O_{12}$ were studied and for each composition the rare earth content was varied according to the formula $(Gd,Y,Ce)_3(Y_XGa_{1-X})_2(Ga,Al)_3O_{12}$; where $-0.01 < X < 0.05$. The visual transparency of the polished ceramics indicated that both yttrium and gallium are necessary to expand the phase stability region. XRD-determined lattice expansions correlated well with the explanation that the phase stability region is due to interionic substitution of the various sized ions between the three cationic garnet lattice sites. The scintillator performance of the gamma ray spectroscopy showed that all the three garnets are suitable materials and offer exceptional energy resolution when compared with other oxides in their class; however, the large phase stability region of the $Gd_{1.5}Y_{1.5}Ga_{2.5}Al_{2.5}O_{12}$ composition makes it especially attractive due to the reduced need for precise chemical control and therefore reduced cost in fabrication and commercialization.

ACKNOWLEDGMENTS

The authors appreciate help from Todd Stefanik of Nanocerox for powder production, Jim Peterson with powder processing, and Patrick Beck for gamma ray spectroscopy. This work has been supported by the US Department of Homeland Security, Domestic Nuclear Detection Office, under competitively awarded IAA HSHQDC-09-x-00208/P00002. This support does not constitute an express or implied endorsement on the part of the Government. This work was performed under the auspices of the U.S. DOE by the Lawrence Livermore National Laboratory under Contract DE-AC52-07NA27344. LLNL-JRNL-653204.

REFERENCES

1. T. Manabe and E. Kazumichi: Crystal growth and optical properties of gadolinium aluminum garnet. *Mater. Res. Bull.* **6**, 1167–1174 (1971).
2. T. Kanai, M. Satoh, and I. Miura: Characteristic of a nonstoichiometric $Gd_{3+\delta}(Al,Ga)_{5-\delta}O_{12}$:Ce garnet scintillator. *J. Am. Ceram. Soc.* **91**, 456–462 (2008).
3. N.J. Cherepy, J.D. Kuntz, Z.M. Seeley, S.E. Fisher, O.B. Drury, B.W. Sturm, T.A. Hurst, R.D. Sanner, J.J. Roberts, and S.A. Payne: Transparent ceramic scintillators for γ spectroscopy and radiography. *Proc. SPIE* **7805**, 780501 (2010).
4. K. Kamada, T. Yanagida, J. Pejchal, M. Nikl, T. Endo, K. Tsutumi, Y. Fujimoto, A. Fukabori, and A. Yoshikawa: Scintillator-oriented combinatorial search in Ce-doped $(Y,Gd)_3(Ga,Al)_5O_{12}$ multicomponent garnet compounds. *J. Phys. D: Appl. Phys.* **44**, 505104 (2011).
5. P. Dorenbos: Electronic structure and optical properties of the lanthanide activated $RE_3(Al_{1-x}Ga_x)_5O_{12}$ (RE=Gd, Y,Lu) garnet compounds. *J. Lumin.* **134**, 310–318 (2013).
6. J.M. Ogiegło, A. Katelnikovas, A. Zych, T. Jüstel, A. Meijerink, and C.R. Ronda: Luminescence and luminescence quenching in $Gd_3(Ga,Al)_5O_{12}$ scintillators doped with Ce^{3+}. *J. Phys. Chem. A* **117**, 2479−2484 (2013).
7. Z.M. Seeley, N.J. Cherepy, and S.A. Payne: Homogeneity of Gd-based garnet transparent ceramic scintillators for gamma spectroscopy. *J. Cryst. Growth* **379**, 79–83 (2013).
8. N.J. Cherepy, Z.M. Seeley, S.A. Payne, P.R. Beck, O.B. Drury, S.P. O'Neal, K. Morales Figueroa, S. Hunter, L. Ahle, P.A. Thelin, T. Stefanik, and J. Kindem: Development of transparent ceramic Ce-doped gadolinium garnet gamma spectrometers. *IEEE Trans. Nucl. Sci.* **60**(3), 2330 (2013).
9. N.J. Cherepy, S.A. Payne, B.W. Sturm, S.P. O'Neal, Z.M. Seeley, O.B. Drury, L.K. Haselhorst, B.L. Rupert, R.D. Sanner, P.A. Thelin, S.E. Fisher, R. Hawrami, K.S. Shah, A. Burger, J.O. Ramey, and L.A. Boatner: Performance of europium-doped strontium iodide, transparent ceramics and bismuth-loaded polymer scintillators. *Proc. SPIE* **8142**, 81420W (2011).
10. J. Kindem, R. Conwell, Z.M. Seeley, N.J. Cherepy, and S.A. Payne: Performance comparison of small GYGAG(Ce) and CsI(TI) scintillators with PIN detectors. *IEEE Nucl. Sci. Sympo., Conf. Rec.* 1621–1623 (2011).
11. J. Nicolas, J. Coutures, and J.P. Coutures: Sm_2O_3-Ga_2O_3 and Gd_2O_3-Ga_2O_3 phase diagrams. *J. Solid State Chem.* **52**, 101–113 (1984).
12. C.D. Brandle and R.L. Barns: Crystal stoichiometry of Czochralski grown rare-earth gallium garnets. *J. Cryst. Growth* **26**, 169–170 (1974).
13. R.D. Shannon: Revised effective ionic radii and systematic studies of interatomic distances in halides and chalcogenides. *Acta Crystallogr.* **A32**, 751–767 (1976).
14. P. Dorenbos: Electronic structure engineering of lanthanide activated materials. *J. Mater. Chem.* **22**, 22344 (2012).
15. J. Ueda, S. Tanabe, and T. Nakanishi: Analysis of Ce^{3+} luminescence quenching in solid solutions between $Y_3Al_5O_{12}$ and $Y_3Ga_5O_{12}$ by temperature dependence of photoconductivity measurement. *J. Appl. Phys.* **110**, 053102 (2011).

https://doi.org/10.1557/jmr.2014.235 Published online by Cambridge University Press